PERFORMANCE ANALYSIS OF 12SLOT-14POLE HEFSM AND FEFSM WITH OUTER-ROTOR CONFIGURATION

M.Z. Ahmad[1*], S.M.S. Othman[2], M.M.A. Mazlan[3], and E. Sulaiman[4,5]

[1,2,3,4]Faculty of Electrical and Electronic Engineering, UTHM, 86400, Batu Pahat, Johor, Malaysia
[5]Research Center For Applied Electromagnetics, UTHM, 86400, Batu Pahat, Johor, Malaysia

ABSTRACT

Recently, research on flux switching machines (FSMs) become an attractive research topic due to several excessive advantages of robust rotor structure, high torque and power capability, and low manufacturing cost that suitable for heavy applications. Nevertheless, most of research have been reported are mainly focused on inner-rotor configuration. The outer-rotor configuration of electric machines are more applicable for direct drive application especially for in-wheel drive electric vehicles (EVs) due to higher torque at low speed and constant power at high operating region. Therefore, this paper presents performance analysis of 12Slot-14Pole hybrid excitation flux switching machine (HEFSM) and field excitation flux switching machine(FEFSM) with outer-rotor configuration. To confirm the machine's operating principles, coil test analysis, magnetic flux characteristics, cogging torque, flux line and torque characteristics at various current densities for both machines are carried out using two-dimensional finite element analysis (2D-FEA). The results obtained show that the HEFSM with outer-rotor configuration has higher torque and power compared with the outer-rotor FEFSM. Since, the machine's performances are still far from the target torque and power, design optimization will be conducted to meet the target for direct drive EV application.

KEYWORDS**:** *Permanent magnet; field excitation coil; flux switching machine; outer-rotor; in-wheel drive.*

1.0 INTRODUCTION

Electric motors with high torque density capability are essential for heavy applications such as in aerospace and automotive area (Zhu & Howe, 2007) Previously, permanent magnet (PM) brushless machines are widely used for these heavy applications due to their advantages of high torque capability. Nevertheless, due to the main flux source of PMs are located on the rotor, the machines are suffer from demagnetization effects which resulting in eddy current loss in the rotor. The main reason on this issue is difficulty to dissolve heat from the rotating part.

* Corresponding Email: zarafi@uthm.edu.my

In recent years, flux-switching motors (FSMs) become an attractive research topic due to several advantages of higher torque density and efficiency. With all active components such as PM, DC field excitation coil (DC FEC), and armature coil are located on the stator, the machine is said very robust in which only consist single piece of rotor. Various applications of FSM have been reported, ranging from wind power generation, automotive, aerospace, power tools and etc (Amara, Hoang, Gabsi, and Lecrivain, 2005; Pollock et al., 2003, 2006; Jin et al., 2010). Generally FSMs can be classified into three groups, namely permanent magnet (PM) FSMs, hybrid excitation (HE) FSMs, and field excitation (FE) FSMs as shown in Figure 1. Both PMFSMs and FEFSMs have only single excitation flux source which come from PM and FE coil, respectively, while in HEFSM the magnetic flux source is generated from both the PM and FECs (Sulaiman, Kosaka, and Matsui, 2011).

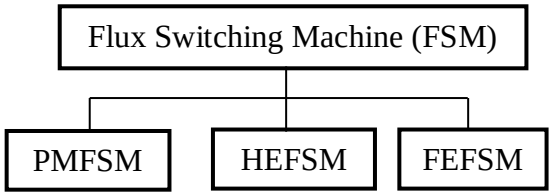

Figure 1. Classification of flux switching machines

However, most of research have been reported are mainly focused on inner-rotor configuration (Xu et al., 2010; Chen & Zhu, 2010; Wang & Deng, 2012; Tang, Paulides, Motoasca &Lomonova, 2012; Sulaiman, 2013; Pollock & Brackley, 2003). It is quite difficult to find any report on outer-rotor FSM. Lately, a report on outer-rotor PMFSM has been published in 2010 and the target of the proposed machine is used for light traction EV applications (Wang, Jin, Shen, Fei, & Luk, 2010; Fei et al., 2012). Nonetheless, with single magnetic flux source of constant PM, it also may suffer from demagnetization effect and uncontrollable flux. Thus, this paper presents performance analysis of 12Slot-14Pole outer-rotor hybrid excitation flux switching machine (HEFSM) and field-excitation flux switching machine (FEFSM) to meet the requirement of in-wheel drive electric vehicle (EV). Previously, the authors have proposed outer-rotor HEFSM, and FEFSM with 12Slot-10Pole configuration in which the initial design has been described in (Ahmad, Sulaiman, Haron, & Kosaka, 2012; Othman & Sulaiman, 2014). Under some design limitations and conditions similar to the conventional interior permanent magnet synchronous machine (IPMSM) employed in existing HEV, 2-D FEA is carried out to analyse and confirm basic operating principle of both machines

The rest of the paper is organized as follows. The machine's design limitations and conditions are described in detail in Section 2.0. The analyses on coil arrangement test, cogging torque, flux path, magnetic flux characteristics and torque characteristics that carried out using 2D-FEA base are demonstrated in Section 3.0. Finally, a conclusion is drawn at the last of the paper to summarize the works have been done.

2.0 DESIGN LIMITATIONS AND CONDITIONS

Initially, the proposed 12slot-14pole HEFSM and FEFSM with outer-rotor configuration are designed using JMAG-Designer 13.0 software. This software is used as 2-D finite element solver for the entire design studies. The initial structure for both machines are depicted in Figure 2 and the number of turns of armature coil and excitation coil are examined by Equation (1) and Equation (2), respectively. Table 1 shows the proposed specifications both machines and the calculated value of N_a, N_e, J_a and J_e.

$$N_a = \sqrt{\frac{\alpha_a R_a S_a}{4\rho L_{a-ave}}} \tag{1}$$

$$N_e = \sqrt{\frac{\alpha_e R_e S_e}{4\rho L_{e-ave}}} \tag{2}$$

From Equation (1), subscript a and e indicating armature coil and excitation coil components, respectively, while N is the number of turns of coil winding, α is the filling factor of coil, R is the coil resistance (Ω), S is the coil slot area (mm^2), and L is the average coil length (mm).

Furthermore, current density of armature coil (J_a) and current density of excitation coil

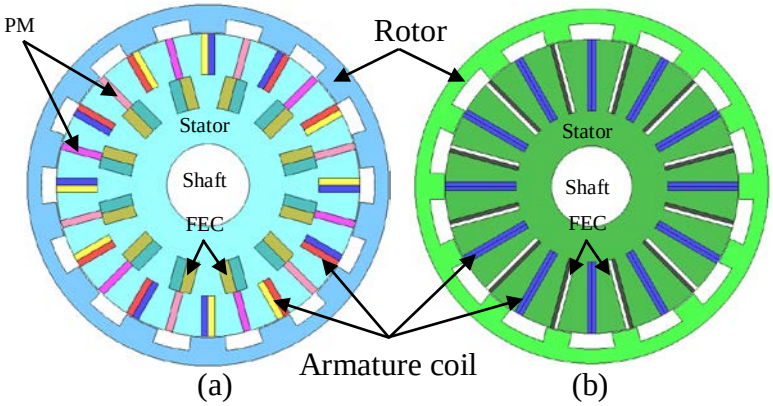

Figure 2. Cross sectional view of initial design machine (a) HEFSM (b) FEFSM

(J_e) for the proposed machine can be determined by Equation (3) and Equation (4), respectively.

$$J_a = \frac{I_a N_a}{\alpha_a S_a} \tag{3}$$

$$J_e = \frac{I_e N_e}{\alpha_e S_e} \tag{4}$$

For the HEFSM, it is composed of 12 PMs and 12 FECs distributed uniformly in the midst of each armature coil, while for FEFSM all PMs as in HEFSM are eliminated and

the space is only accomodates with FECs. The term, "flux switching", is created to describe machines in which the stator tooth flux switches its polarity by following the motion of a salient pole rotor. In this 12Slot-14Pole machine, the PMs and/or FECs produce six north poles interspersed between six south poles. The three-phase armature coils are accommodated in the 12 slots for each 1/4 stator body periodically. As the rotor rotates, the fluxes generated by PMs and/or mmf of FECs link with the armature coil alternately. For the rotor rotation through 1/14 of a revolution, the flux linkage of the armature has one periodic cycle and thus, the frequency of back-emf induced in the armature coil becomes fourteen times of the mechanical rotational frequency. Generally, the relation between the mechanical rotation frequency and the electrical frequency for both machines can be expressed as in Equation (5).

$$f_e = N_r f_m \tag{5}$$

where f_e is the electrical frequency, f_m is the mechanical rotation frequency and N_r is the number of rotor poles, respectively.

Table 1. Specifications of both HEFSM/FEFSM

Armature coil slot		**Field excitation coil slot**	
α_a	0.6/0.5	α_e	0.6/0.5
R_a	1 Ω	R_e	1 Ω
S_a	147.08 mm^2	S_e	197.51 mm^2 (HEFSM) and 168mm^2 (FEFSM)
ρ	1.673E-08 Ωm	ρ	1.673E-08 Ωm
N_a	7 turns	N_e	44 turns
J_a	30 A/mm^2	J_e	30 A/mm^2

The design limitations and conditions for both machines are set similar with the conventional interior permanent magnet synchronous motor (IPMSM) employed in existing HEV (Ahmad et al., 2013). The maximum torque and power of 333Nm and 123kW, respectively is set as the target performances. On the other hand, the total PM volume for HEFSM is reduced to 1.0kg, while for FEFSM there is no PM et al in order to reduce the manufacturing cost. Furthermore, 30A/mm^2 is set as the maximum current density of both armature coil and excitation coil, while the voltage and current limitation for the inverter is 650V and 360A_{rms}, respectively. With all active components are in rectangle shape resulting for easier in manufacturing and optimization process. Consequently, the proposed machine is expected has low copper loss for HEFSM due to no overlap windings between the armature and FECs coil resulting for higher efficiency. Finally, both machines are expected to have maximum torque and power densities of 11.1Nm/kg and 4.1kW/kg for HEFSM, while 3kW/kg and 6Nm/kg for FEFSM, respectively.

The proposed machines consist of 24 stator teethes with alternate DC FEC, PM and armature coil slot around the stator body. Initially, the DC FEC is wound alternately in counter-clockwise and clockwise polarity, while all the three- phase armature coils are wound in counter-clockwise direction. Furthermore, the material used in this design for

PM is NEOMAX-35AH whose residual flux density and coercive force at 20ºC 1.2T and 932kA/km, respectively, while the electromagnetic steel of 35H210 is used for the

Table 2. Initial dimension of the machines

Parameters	HEFSM	FEFSM
Inner rotor radius (mm)	111.4	110.36
Rotor pole depth (mm)	10.3	10.82
Rotor pole arc span (º)	12.86	11.35
PM slot depth (mm)	30	Nil
PM slot width (mm)	2.63	Nil
FEC slot depth (mm)	23.88	53.04
FEC slot width (mm)	8.25	2.77
Armature coil slot depth (mm)	28.35	53.04
Armature coil slot width (mm)	4.95	3.17
Shaft radius (mm)	30	30

rotor and stator iron core. The dimension of the initial design for both machines are depicted in Table 2.

3.0 PERFORMANCE ANALYSIS BASED ON 2D-FEA

3.1 Armature Coil Arrangement Test

Initially, it is essential to perform the operating principle of the proposed machine by conducting a coil arrangement test on each of the armature coil. The appropriate polarity and coil phase of armature coil must be examined and identified to confirm the proposed machine be able to operate properly. Firstly, the polarity of all the armature coils are set in counter clockwise direction, while the DC FEC and/or PM polarities are set in alternate direction in order to provide 12 north and 12 south poles, respectively. By injected zero current into DC FEC in which the FEC current density is 0 A/mm^2 (for the case of HEFSM), the flux linkages on each armature coil are analyzed. Simultaneously, the generated magnetic fluxes on each armature coil are compared.

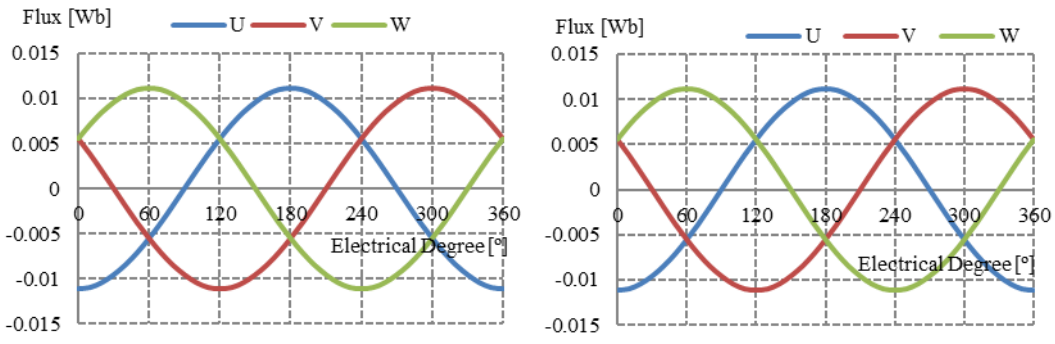

(a) (b)

Figure 3. Three-phase magnetic flux (a) HEFSM (b) FEFSM

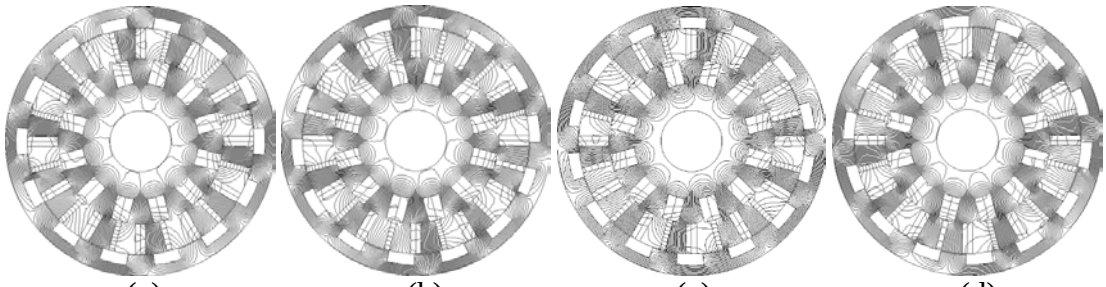

(a) (b) (c) (d)

Figure 4. HEFSM PM flux path at various rotor position, (a) 0º, (b) 9º, (c) 18º, (d) 27º

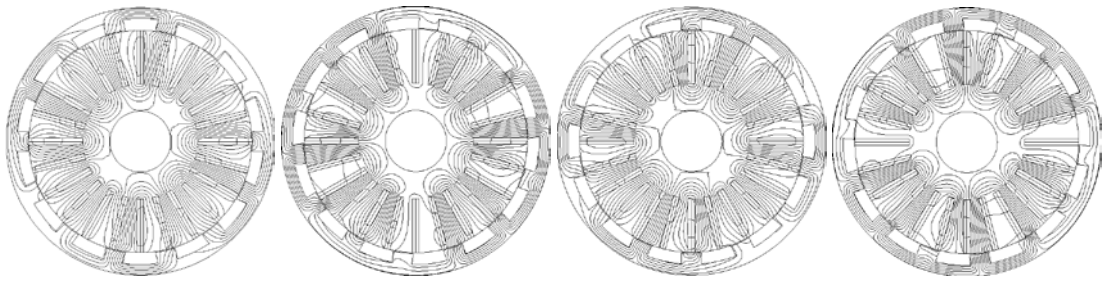

(a) (b) (c) (d)

Figure 5. FEFSM mmf of FEC flux path at various rotor position, (a) 0º, (b) 9º, (c) 18º, (d) 27º

Then, the fluxes profiles that have same pattern and phase angle are categorized into a same phase. The three-phase of 12 armature coils are examined based on normal balance three-phase 120º phase shifted. From the coil arrangement test, results of three-phase magnetic flux for both machines are illustrated in Figure 3. It is obvious that the maximum amplitude of both magnetic flux generated by PM only of HEFSM and the maximum mmf of FECs of FEFSM at maximum FEC current density is 0.011 Wb. In addition, both machines have solidly sinusoidal of magnetic flux and expected that have less harmonics effect.

3.2 Flux Path

The flux path due to PM source for HEFSM is also investigated at different rotor position. Figure 4 shows the flux path of PM at 0º, 9º, 18º, and 27º rotor position. It is obvious that, 50% of the PM flux flows from stator to rotor while the remaining flux flows around the DC FEC slot to form a complete 12 cycles of flux. However, very high flux density occurs between the adjacent of FEC slot and between the lower edge of armature coil and upper edge of DC FEC slots which results in flux saturation. Therefore, the appropriate distance between them needs to be examined to minimize the flux saturation effect to give optimal torque and power performances.

On the other hand, the mmf FEC flux path of FEFSM is depicted in Figure 5. It is observable that almost 50% of fluxes are also flows from stator to the rotor. Nonetheless, since the PMs are eliminated from the stator body, there is no flux saturation occurs.

3.3 Cogging Torque

The cogging torque of the proposed machine in open circuit condition is illustrated in Figure 6. It is observed within 36º of rotor position which is one electric cycle and clearly seen that there is six cycles of peak-to-peak cogging torque. It is obvious that, the FEFSM has lower peak-to-peak cogging as compared with HEFSM with the maximum of 4.11Nm and 7.99Nm, respectively. However, the peak-to-peak cogging torque of HEFSM has posibility to be reduced by conducting an optimization process. This phenomenon is due to flux saturation on the region between the FEC slot and armature coil slot that prevent the flux flows smoothly.

3.4 Flux Characteristics at Various Current Densities

The flux linkage of PM and various DC FEC current densities for HEFSM are demonstrated in Figure 7(a), while for FEFSM is plotted in Figure 7(b). It is obvious that for HEFSM when DC FEC current density, J_e start increased, the flux linkage also increasing and reach to maximum when Je set to 10A/mm^2. The maximum flux linkage at this condition is approximately 0.051Wb which is increased more than three times when compared with flux linkage come from PM only. When further increased of J_e, the flux linkage starts to reduce and finally when J_e is set to maximum of 30A/mm^2, the magnitude of flux linkage is approximately 0.028 Wb. This phenomenon is expected due to flux saturation when higher J_e is injected to the system beyond 10 A/mm^2. However, this analysis has proved that the additional DC FEC can improve the generated flux from PM and offers variable flux control capability.

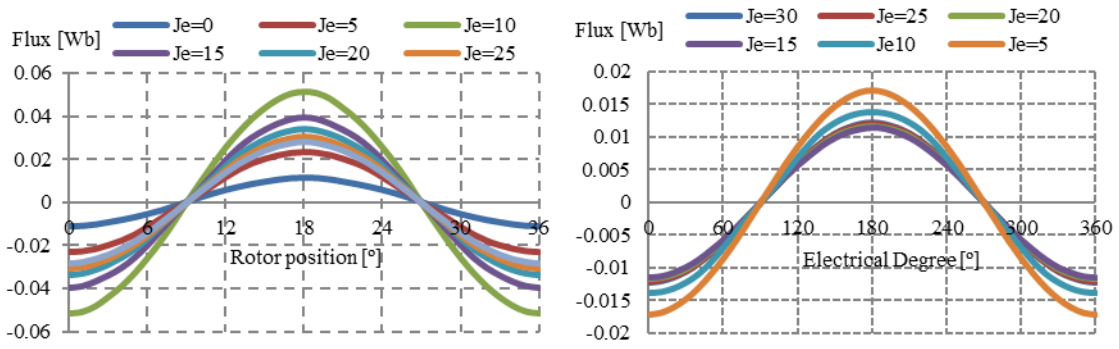

(a) HEFSM (b) FEFSM

Figure 7. Flux characteristics at various FEC current densities

For FEFSM, it is clearly seen that almost similar pattern as HEFSM was recorded but the maximum flux of 0.018Wb is reached when J_e is set at 5A/mm^2. When J_e is further increased, the magnitude of flux start to reduce and at maximum of J_e, the magnitude of flux is only 0.013Wb.

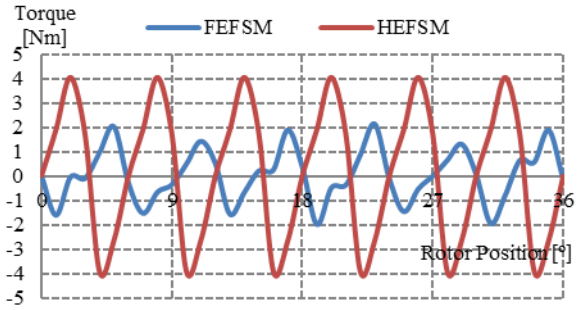

Figure 6. Cogging torque

3.5 Torque Characteristic at Various Current Densities

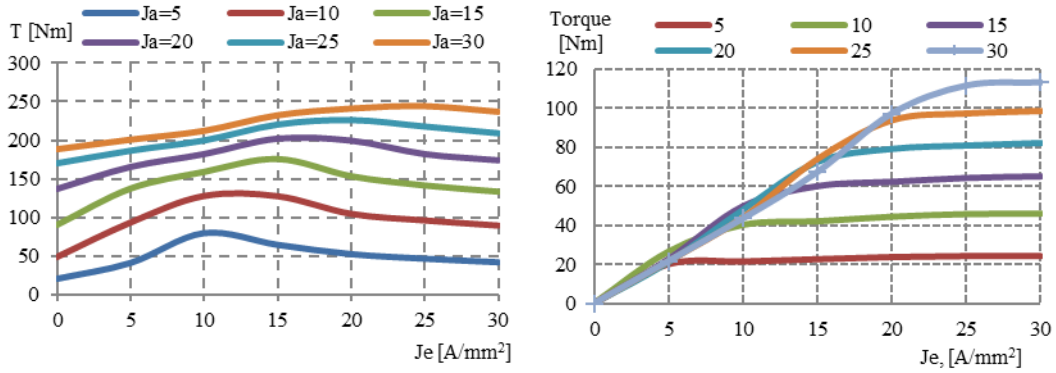

(a) HEFSM (b) FEFSM

Figure 8. Torque characteristics at various FEC current densities

The torque characteristics at various armature current density and DC FEC current density are also investigated. The results obtained is plotted in Figure 8(a) and Figure 8(b) for HEFSM and FEFSM, respectively. Both the armature current and FEC current densities is varied from 0 to 30A/mm^2. The graph show that the maximum average torque 243.52Nm of initial design machine for HEFSM is obtained when armature and FEC current densities are set to 30A$_{rms}$/mm^2 and 25A/mm^2. Whislt, the maximum average torque of 112.95 Nm for FEFSM is also obtained at the same condition maximum J_a and J_e. Whereas, the maximum power obtained for the HEFSM and FEFSM is 83.03 kW and 50.46kW, respectively. Therefore, the optimal torque and power of both machines are expected can be improved by implementing design optimization using a conventional deterministic optimization method.

4.0 CONCLUSION

This paper has discussed and demonstrated the initial performances of 12slot-14pole outer-rotor HEFSM and FEFSM. The research goal is to determine the initial result such as flux linkage, cogging torque, average and maximum torque, flux line and power as the primary condition before further research. It can be concluded that HEFSM with outer-rotor configuration have higher average torque and power compared with outer-rotor FEFSM, hence suitable for heavy application such as in EV/HEV propulsion

system. To achieve optimal performances, further design investigation and improvement will be conducted through deterministic optimization approach to meet the target torque and power for direct drive application.

ACKNOWLEDGEMENT

This research was supported by University Tun Hussein Onn Malaysia (UTHM) and Ministry of Education Malaysia (MOE).

REFERENCES

Ahmad, M.Z., Sulaiman, E., Haron, Z.A., & Kosaka, T. (2012). Preliminary Studies on a New Outer-Rotor Permanent Magnet Flux Switching Machine with Hybrid Excitation Flux for Direct Drive EV Applications. IEEE International Power and Energy Conference (PECON2012), 928-933.

Ahmad, M. Z., Sulaiman, E., Haron, Z. A., & Kosaka, T. (2013). Impact of rotor pole number on the characteristics of outer-rotor hybrid excitation flux switching motor for in-wheel drive EV. *Procedia Technology*, 11: 593-601.

Amara, Y., Hoang, E., Gabsi, M., & Lecrivain, M. (2005). Design and comparison of different flux-switching synchronous machines for an aircraft oil breather application. *European Transaction on Electrical Power*, 15: 497-511.

Chen, J.T., & Zhu, Z.Q., (2010). Winding configuration and optimal stator rotor pole combination of flux-switching PM brushless machines. *IEEE Transaction on Energy Conversion*, 25: 293-302.

Fei, W., Chi, P., Luk, K., Shen, J. X., Wang, Y., & Jin, M. (2012). A Novel Permanent-Magnet Flux Switching Machine With an Outer-Rotor Configuration for In-Wheel Light Traction Applications. *IEEE Transactions on Industry Applications*, 48(5): 1496–1506.

Jin, M. J., Wang, Y., Shen, J.X, Luk, P.C.K, Fei, W.Z., & Wang, C.F. (2010). Cogging torque suppression in a permanent magnet flux-switching integrated starter generator. *IET Electric Power Applications*, 4(8): 647-656.

Othman, S.M.N.S., & Sulaiman, E., (2014). Design study of 3-phase field-excitation flux switching motor with outer-rotor configuration. IEEE Power Engineering and Optimization Conference (PEOCO 2014), 330-334.

Pollock, C. & Brackley, M. (2003). Comparison of the acoustic noise of flux-switching and switched reluctance drive. *IEEE Transaction on Industry Applications*, 39(3): 826-834.

Pollock, C., Pollock, H., Borron, R., Coles, J. R., Moule, D., Court, A., & Sutton, R. (2006). Flux-switching motors for automotive applications. *IEEE Transaction on Industry Applications*, 42(5): 1177-1184.

Pollock, H., Pollock, C., Walter, R.T., & Gorti, B.V. (2003). Low cost high power density, flux switching machines and drives for power tools. IEEE Industry Applications Soc. Annu. Meeting, 1451-1457.

Sulaiman, E., Kosaka, T., & Matsui, N. (2011). High power density design of 6slot-8pole hybrid excitation flux switching machine for hybrid electric vehicles. *IEEE Transaction on Magnetics*, 47(10): 4453-4456.

Sulaiman, E., Ahmad, M. Z., Kosaka, T., & Matsui, N. (2013). Design Optimization Studies on High Torque and High Power Density Hybrid Excitation Flux Switching Motor for HEV. *Procedia Engineer*ing, 53: 312-322.

Tang, Y., Paulides, J.J.H., Motoasca, T.E., & Lomonova, E.A. (2012). Flux-switching machine with DC excitation. *IEEE Transaction on Magnetics*, 48(11): 3583 - 3586.

Wang, Y., & Deng, Z. (2012). Comparison of hybrid excitation topologies for flux-switching machines. *IEEE Transaction on Magnetics*, 48(9): 2518 – 2527.

Wang, Y., Jin, M.J., Shen, J., Fei, W.Z., & Luk, P.C.K. (2010). An outer-rotor permanent magnet flux-switching machine for traction application. Energy Conversion Congress and Expo-sition (ECCE), 1723-1730.

Xu, W., Zhu, J., Zhang, Y., Wang, Y., Li, Y., & Hu, J. (2010). Flux-switching permanent magnet machine drive system for plug-in hybrid electrical vehicle. IEEE Conference on Australian Universities Power Engineering (AUPEC), 1-6.

Zhu, Z. Q., & Howe, D. (2007). Electrical machines and drives for electric, hybrid, and fuel cell vehicles. Proceedings of the IEEE, 95(4): 746-765.